ASEAN Journal of Chemical Engineering 2026, Vol. 26, No. 2,313 – 329

Synthesis of Graphite/NiO/G-OH (Nickel Oxide/Hydroxyl-Functionalized Graphene) Nanocomposite Electrode for the Electro-degradation of Remazol Black 5 (RB5) Dye

Ni Made Wiratini [*,1]
Siti Maryam [1]
I Ketut Lasia [1]
Dewa Ketut Sastrawidana [1]
Ni Luh Putu Ananda Saraswati [1]
Khusna Arif Rakhman [2]
Indra Cipta [2]
[1] *Department of Chemistry, Faculty of Mathematics and Natural Sciences, Ganesha University of Education, Singaraja 81116, Indonesia*
[2] *Department of Chemistry Education, Faculty of Mathematics and Natural Sciences, Universitas Khairun, Ternate 53, Indonesia*
*e-mail: made.wiratini@undiksha.ac.id

Submitted 23 October 2025 *Revised* 15 April 2026 *Accepted* 18 April 2026

Abstract. Hydroxyl-functionalized graphene (G–OH) is a graphene material containing hydroxyl (–OH) as its main functional group. A higher quantity of –OH group indicates a more electroactive oxide nature, which is highly beneficial for the electrochemical degradation of remazol black 5 (RB5). Graphite electrodes, commonly used as anodes for the oxidation of organic compounds, are composed of carbon; however, they exhibit low oxidation activity toward organic compounds and are susceptible to corrosion. Therefore, deposition of a NiO/G–OH electrocatalyst on the graphite surface is necessary to enhance both activity and stability. The G–OH synthesis was carried out using a combination of electrochemical exfoliation and ultrasonication. The graphite/NiO/G–OH electrodes were prepared by electrodeposition of NiO from a solution of $NiSO_4 \cdot 6H_2O$ and G–OH at pH 10. Both graphite and graphite/NiO/G–OH electrodes were characterized using FTIR and SEM–EDX analyses. The electrochemical degradation performance of graphite and graphite/NiO/G–OH electrode was evaluated for the degradation of RB5 under varying time, pH, and NaCl concentration conditions. FTIR and SEM–EDX characterization confirmed the successful deposition of NiO/G–OH on the graphite electrode. The optimum conditions for RB5 degradation using the graphite electrode were pH 4, 9 V, 0.10 M NaCl, and a reaction time of 60 minutes, resulting in a 94.05% reduction in absorbance. In comparison, the graphite/NiO/G–OH electrode achieved complete degradation (100% absorbance reduction) under the same pH and voltage conditions, using 0.05 M NaCl for 60 minutes. GC–MS analysis of the degradation products revealed the presence of cyclic, aromatic, and organic acids, indicating the effective breakdown of the dye molecules. Based on these findings, graphene-based electrodes show strong potential as efficient, environmentally friendly materials for the electrochemical degradation of organic pollutants.

Keywords: Electro-degradation, Electrode, Graphite/NiO/G-OH, Remazol black 5

DOI: 10.22146/ajche.25031

INTRODUCTION

Dyes are colored organic compounds or mixtures used to impart color to materials such as textiles, paper, plastics, and leather. The dyed materials must be resistant to washing, and the dyes should also exhibit stability to light (Samarghandi *et al.*, 2020). Industrial dyes commonly include azo derivatives (–N=N–), anthraquinones, indigoids, triphenylmethyls, xanthenes, and sulfur-based compounds (Vasconcelos *et al.*, 2019). Among these, synthetic dyes are widely used, particularly in the textile dyeing industry. One of the most commonly used dyes is remazol black 5 (RB5). Reduction of its azo bond (–N=N–) highly carcinogenic amine compounds (Nidheesh *et al.*, 2018). Textile effluents contribute significantly to river pollution, accounting for approximately 10–15% (m/v) of total contamination, with up to 50% of this waste containing RB5. Therefore, simple and efficient methods are urgently needed to treat textile wastewater. One effective approach to convert dye pollutants into environmentally safe species is oxidative electro-degradation (Kim & Jo, 2019).

Electro-degradation is an effective wastewater treatment method widely used for dye degradation of (Gündüz & Atabey, 2019). Its advantages include a simple process, adjustable operating conditions at atmospheric pressure and room temperature, and the production of environmentally benign end products such as CO_2 and H_2O (Migliorini *et al.*, 2016; Cornejo *et al.*, 2019). A common challenge in electro-degradation reactions is the selection of electrode materials suitable for specific reaction conditions (Ajeel *et al.*, 2016). Various electrodes have been employed as anodes for dye degradation, including boron-doped diamond (Migliorini *et al.*, 2016) and Ti/SnO_2-IrO_2 (Bravo-Yumi *et al.*, 2020). However, these electrodes are very expensive, making them less practical for large-scale wastewater treatment applications. In addition, their degradation efficiency is relatively low (Yusbarina *et al.*, 2021).

To overcome these limitations, electrode modification is necessary. Such modification can be achieved by adding a substrate or through metal doping, which acts as a catalyst (Kaur *et al.*, 2018). Surface modification of electrodes can enhance their activity and stability, accelerate the degradation rate of pollutant compounds, and improve the overall efficiency of electrochemical processes by reducing electrical energy consumption during wastewater treatment (Zhang *et al.*, 2019).

Carbon-based materials are suitable candidates for anode modification in wastewater treatment due to their high electrical conductivity, abundance, and non-toxicity. Among them, graphene stands out as a promising modifier because of its excellent mechanical strength, high thermal and electrical conductivity, attractive optical properties, large surface area, good catalytic performance, and corrosion resistance (Safarpour & Khataee, 2018). Functionalization of graphene with oxygen-containing functional groups to form graphene oxide (GO) and reduced graphene oxide (rGO) has demonstrated high electrocatalytic performance in dye degradation (Saroyan *et al.*, 2019; Li *et al.*, 2019). However, the presence of multiple oxygen-containing functional groups, each highly reactive, makes the functionalization process difficult to control (Shetti *et al.*, 2019). This complexity can negatively affect the graphene's intrinsic properties, leading to reduced conductivity, structural defects, and reduced thermal and mechanical stability

(Vacchi *et al.*, 2018).

Therefore, it is crucial to design graphene-based materials with tailored functional groups for specific applications. The introduction of a single functional group can modify the electronic bonding states of graphene (Jung *et al.*, 2021). Functionalization of graphene with hydroxyl groups yields hydroxyl-functionalized graphene (G–OH), which contains numerous hydroxyl groups within its structure. These groups play a key role in determining the material's reactivity during dye electro-degradation.

Previous studies on the electrochemical oxidation of dyes using graphene have demonstrated promising results. For example, the electrochemical oxidation of 10 $mg.L^{-1}$ reactive black 5 (RBk5) using a graphene anode (GN)/TiO_2 in a 1 $g.L^{-1}$ NaCl supporting electrolyte for 60 min showed that the removal efficiency of RBk5 could exceed 95% (Li *et al.*, 2019). In another study, the electrochemical oxidation of 20 $mg.L^{-1}$ methylene blue using an SS/G-OH electrode in a 0.05 M NaCl electrolyte showed that the methylene blue (MB) concentration decreased by more than 99% after 30 min of electrolysis (Yusbarina *et al.*, 2021). Furthermore, the electrochemical oxidation of 25 $mg.L^{-1}$ MB using G/SnO_2 and G/Sb-SnO_2 electrodes in a 0.5 M Na_2SO_4 electrolyte showed removal efficiencies of 35% and 40%, respectively, within 12 min. Despite these promising results, GN/TiO_2 and SS/G-OH electrodes suffer from limitations, including ohmic losses during regeneration and high energy consumption (Sharif & Roberts, 2020).

The rate of electro-degradation reactions depends on the concentration of electroactive species at the electrode surface. The use of G–OH as an anode modifier can generate large amounts of hydroxyl radicals (•OH) in solution, which act as powerful oxidizing agents. These radicals are highly reactive toward organic compounds and can effectively degrade them (Moreira *et al.*, 2017). Moreover, when NaCl is used as a supporting electrolyte, G–OH can further oxidize Cl^- ions to Cl_2, another strong oxidizing agent. This synergistic effect enhances the electrocatalytic performance of G–OH as an electrode modifier in the electro-degradation of organic pollutants.

Graphite is one of the most commonly used electrode materials (Brillas & Martínez-Huitle, 2015). However, graphite electrodes suffer from several drawbacks, including a high corrosion rate, low mineralization efficiency, and poor oxidation activity toward organic compounds (Shestakova & Sillanpää, 2017). To overcome these limitations, graphite modification is necessary. Nickel oxide (NiO) is a promising anode material for the oxidation of organic compounds (Basharat *et al.*, 2015). It serves as an excellent electrocatalyst, offering better performance compared to Pt or RuO_2, while also being environmentally friendly and cost-effective (Dar *et al.*, 2013). NiO has high overpotential, stability, electrical conductivity, and high catalytic activity (Ding *et al.*, 2016). The incorporation of transition metal oxides into graphite is a promising approach to enhance catalytic activity (Brillas & Martínez-Huitle, 2015).

Composite electrocatalysts exhibit higher activity than single-component electrocatalysts because they possess a larger surface area (Zhang *et al.*, 2019), greater hardness, and enhanced corrosion resistance (Ramalingam, 2019). Ni–SiO_2/carbon paper composite electrodes exhibited high specific surface area, catalytic activity, and stability in the electrooxidation of hydrogen peroxide (Zhang *et al.*, 2019).

This study builds on previous research (Wiratini *et al.*, 2023), which investigated the electrodeposition of NiO/G–OH nanocomposite electrocatalysts on graphite electrode surfaces to overcome the limitations of conventional graphite electrodes and to enhance their catalytic activity and stability. The graphite/NiO/G–OH (nickel oxide/hydroxyl-functionalized graphene) nanocomposite electrodes were then applied to the electro-degradation of RB5 dye. The parameters investigated included the electro-degradation time, solution pH, and the concentration of the NaCl electrolyte. The NiO/G–OH electrocatalyst composite deposited on graphite can significantly improve its properties and enhance its electrochemical performance, making it a promising material for applications in household and medium-scale textile wastewater treatment.

MATERIALS AND METHODS

Materials

The chemicals used in this study included Na_2SO_4 (99% purity, Merck, Germany), graphite electrode (99.9%), $NiSO_4{\cdot}6H_2O$ (>98%, Sigma-Aldrich), KCl (99.5% purity, Merck, Germany), KOH (85% purity, Merck, Germany), NaCl (≥99.5%, Sigma-Aldrich), HCl (37–38% purity, Merck, Germany), remazol black 5 (≥50%, Sigma-Aldrich), and acetone (Merck, Germany).

Synthesis and Characterization of G-OH

The preparation of graphite electrodes was carried out in the following stages: a cylindrical graphite electrode with a diameter of 10 mm and a length of 5 cm was immersed in 50 mL of a solution consisting of 10 mL of 0.003 M H_2SO_4 and 40 mL of 30% H_2O_2 (1:4 ratio) for 15 minutes. The graphite electrode was then removed from the solution and oven-dried at 110°C for 2 hours. Subsequently, it was cooled in a desiccator and weighed using a digital analytical balance. The prepared graphite electrode was then ready for use in the synthesis of G–OH and graphite/NiO/G–OH.

The G–OH synthesis was carried out using a combination of electrochemical exfoliation and ultrasonication methods. The electrochemical cell consisted of graphite anode and cathode electrodes with diameters of 10 mm and lengths of 5 cm. The two graphite electrodes were arranged in parallel, separated by 1 cm, and 3.5 cm of each electrode was immersed in 50 mL of 1 M Na_2SO_4 electrolyte solution. The electrodes were connected to a 10 V DC power supply, and the electrolysis was conducted for 120 minutes. The products obtained by electrochemical exfoliation were filtered, washed three times with distilled water, dried at 80 °C for 1 hour, and weighed. The weights of the cathode and anode before and after the electrochemical exfoliation process were also measured. Subsequently, the ultrasonication process was performed by dispersing 0.20 g of the electrolysis solid in 100 mL of a water–acetone mixture (25:75 v/v). The mixture was sonicated for 120 minutes and then dried at 80°C to obtain the solid G–OH. The G–OH solid was characterized for its functional groups using FTIR spectrophotometry, while its surface morphology, microstructure, and elemental composition were analyzed using SEM–EDX.

Synthesis and Characterization of Graphite/NiO/G-OH Electrodes

The graphite/NiO/G–OH electrodes were synthesized via electrodeposition of Ni and G–OH. A total of 50 mL of deposition solution containing 10 mL of 0.5 M $NiSO_4{\cdot}6H_2O$, 30 mL

of 0.1 M KCl, 10 mL of 0.1 M KOH, and 0.20 g of G–OH was stirred for 30 minutes at 100 rpm. Electrodeposition was performed at pH 10, using graphite electrodes as both the anode and cathode, with 3.5 cm of each electrode immersed in the solution and a 1 cm gap between them. The process was carried out using a DC power supply at 1 V for 300 minutes at 25-30 °C. The resulting graphite/NiO/G–OH electrode was then heated at 400°C for 30 minutes. The electrode surface morphology was characterized by SEM–EDX, and its chemical structure was confirmed by FTIR spectroscopy.

Electro-degradation of RB5 Using Graphite/NiO/G-OH Electrodes

Electro-degradation of RB5 was performed using a graphite/NiO/G–OH nanocomposite anode to optimize key operational parameters, including reaction time, pH, and NaCl concentration. The experiments were conducted using 125 mL of solution containing RB5 dye and the NaCl electrolyte, placed in a 250 mL Pyrex beaker. A DC power supply providing 9 V was applied, and the initial dye concentration was maintained at 300 ppm. Optimization of the electro-degradation process was carried out under varying conditions: time (15, 30, 45, 60, and 90 minutes), pH (4, 6, and 8), and NaCl concentration (0.05, 0.10, 0.25, and 0.50 M). The RB5 solutions before and after electro-degradation were analyzed using UV–Vis spectrophotometry and GC–MS to determine degradation efficiency and identify degradation products.

RESULTS AND DISCUSSION

Synthesis and Characterization of G-OH

The electrochemical exfoliation method was conducted in an electrochemical cell with a simultaneous anodic–cathodic exfoliation design, enabling concurrent exfoliation at both electrodes. High-purity graphite was used as the electrode material, and Na_2SO_4 served as the electrolyte solution.

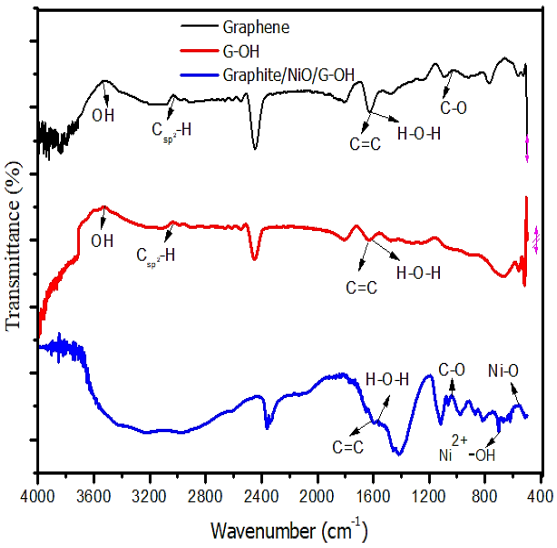


Fig. 1: FTIR spectra of graphene, G-OH, and graphite/NiO/G-OH

Exfoliation of graphite at the anode and cathode in the Na_2SO_4 electrolyte involved the intercalation of Na^+ ions at the cathode and SO_4^{2-} ions at the anode, leading to the exfoliation of graphite into graphene layers. These findings are consistent with previous research, which reported that, during anodic exfoliation, salt electrolytes containing ClO_4^-, Cl^-, and NO_3^- anions do not exhibit exfoliation in contrast, those containing SO_4^{2-} anions demonstrate efficient exfoliation (Parvez *et al.*, 2015).

Most graphite exfoliation occurs at the anode, where oxidation takes place. The SO_4^{2-} ions are attracted to the anode and intercalate between the graphite layers, increasing the interlayer distance (Parvez *et al.*, 2014). In addition to sulfate ions, OH^- ions generated from water oxidation also intercalate into the graphite layers. Water oxidation produces OH^- ions, which are

further oxidized to form oxygen radicals. This intercalation process leads to the exfoliation of graphite into few-layer or single-layer graphene.

The graphene obtained from electrochemical exfoliation was subjected to ultrasonication using a water–acetone solvent mixture (25:75 v/v). The use of this solvent provides a safe dispersion medium with a low boiling point, allowing oxidation to occur during ultrasonication and enabling the resulting G–OH dispersion to be deposited onto the graphite surface.

The ultrasonication process enhances graphite exfoliation by providing additional energy to overcome the van der Waals forces between layers (Htwe *et al.*, 2019). Moreover, transient cavitation during ultrasonication in aqueous solutions generates hydrogen atoms and hydroxyl radicals, which can react with dissolved species (Thaneswari & Lourduraj, 2017). In this study, hydroxyl radicals generated during ultrasonication oxidize graphene forming G–OH. In the first step, electrochemical exfoliation of graphite yields graphene, which may be partially oxidized during the process to produce oxidized graphene. In the second step, ultrasonication of this partially oxidized graphene in a 75% acetone solution results in the formation of G–OH.

The FTIR spectra of graphene, G–OH, and graphite/NiO/G–OH are presented in Figure 1. The FTIR spectrum of graphene obtained through electrochemical exfoliation shows the presence of oxygen-containing functional groups (Chow *et al.*, 2023). The broad peak at 3,448 cm^{-1} corresponds to the O–H stretching vibration, while the peak at 1,635 cm^{-1} is attributed to C=C and H–O–H stretching vibrations. A small peak at 3,050 cm^{-1} indicates the Csp^2–H stretching vibration. All observed FTIR peaks are consistent with the characteristic features of graphene and G–OH structures. The C–O stretching vibration at 1,126 cm^{-1} was identified in graphene, whereas the corresponding peak in G–OH was not observed. These findings are consistent with previous studies (Yan *et al.*, 2012).

Figure 2 shows the SEM and EDX results of graphene and G–OH. The SEM–EDX analysis of the electrochemically exfoliated graphite confirms the formation of oxidized graphene with elemental compositions of 82.20% C and 17.80% O. After the sonication process, hydroxyl groups were introduced onto the graphene surface, resulting in hydroxyl-functionalized graphene (G–OH) with compositions of 81.00% C and 19.00% O.

The FTIR spectrum of the graphite/NiO/G–OH electrode in Figure 1 shows a peak at 1,635 cm^{-1} corresponding to the C=C and H–O–H stretching vibrations. The presence of the C–O bond is confirmed by the peak at 1,126 cm^{-1}. The peaks observed at 700 cm^{-1} and 501 cm^{-1} are attributed to Ni^{2+}–OH and Ni–O stretching vibrations, respectively (Rebelo *et al.*, 2019). These results confirm that NiO/G–OH has been successfully deposited on the graphite electrode surface.

The successful coating of NiO/G–OH on the graphite electrode was confirmed by SEM-EDX analysis. As shown in Figure 3, the graphite/NiO/G–OH electrode exhibits a porous morphology, with the entire graphite surface uniformly covered by the NiO/G–OH layer. The porous structure is crucial for facilitating the transfer of pollutants during the degradation process (Li *et al.*, 2017). The elemental composition obtained from EDX analysis indicates the presence of C (80.10%), O (18.20%), and Ni (1.70%), confirming that C and O originate from G–OH, while Ni is derived from NiO.

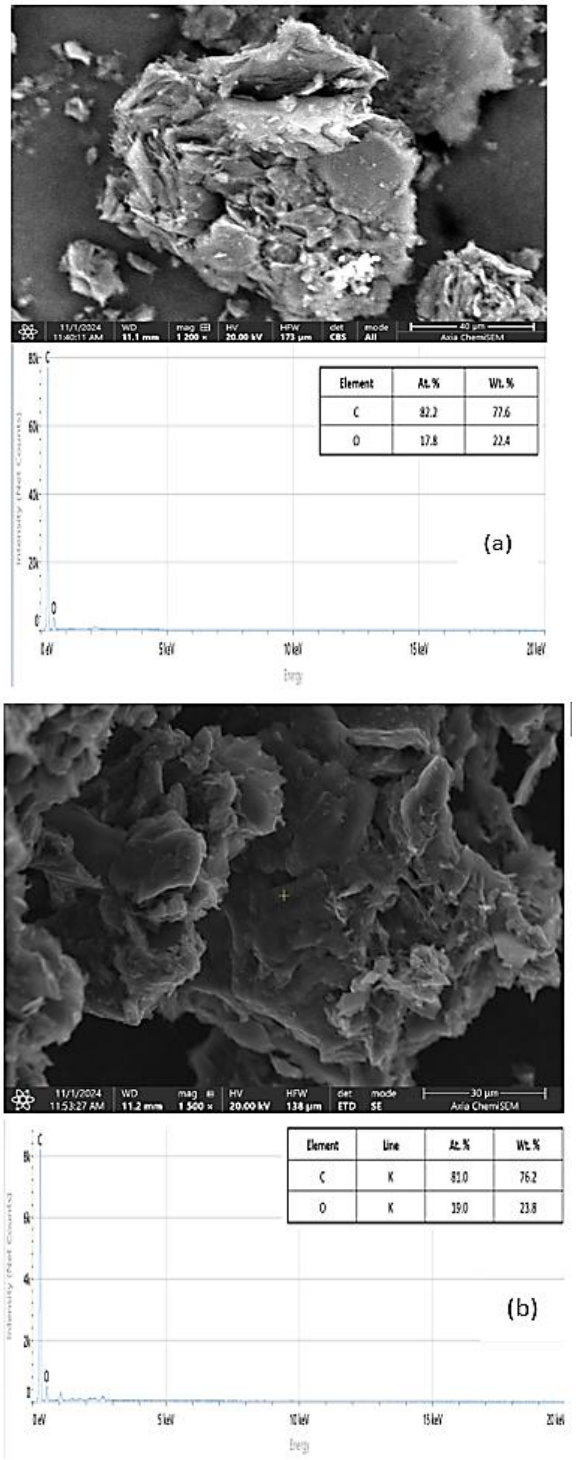


Fig. 2: SEM-EDX of graphene (a) and G-OH (b)

Synthesis and characterization of graphite/NiO/G-OH electrode

Electro-degradation of RB5 Using Graphite/NiO/G-OH Electrodes

The electro-degradation of RB5 dye using graphite and graphite/NiO/G–OH electrode was conducted under various reaction times, pH values, and NaCl concentrations. As shown in Figure 4, the UV–Vis spectrum of RB5 exhibits five characteristic absorbance peaks. The major peak at 595 nm corresponds to the chromophoric –N=N– (azo) group, in contrast the peaks at 229, 254, 310, and 391 nm are associated with unsaturated structures such as benzene, naphthalene, and heterocyclic rings (Droguett *et al.*, 2020; Rivera *et al.*, 2011; Tang *et al.*, 2020).

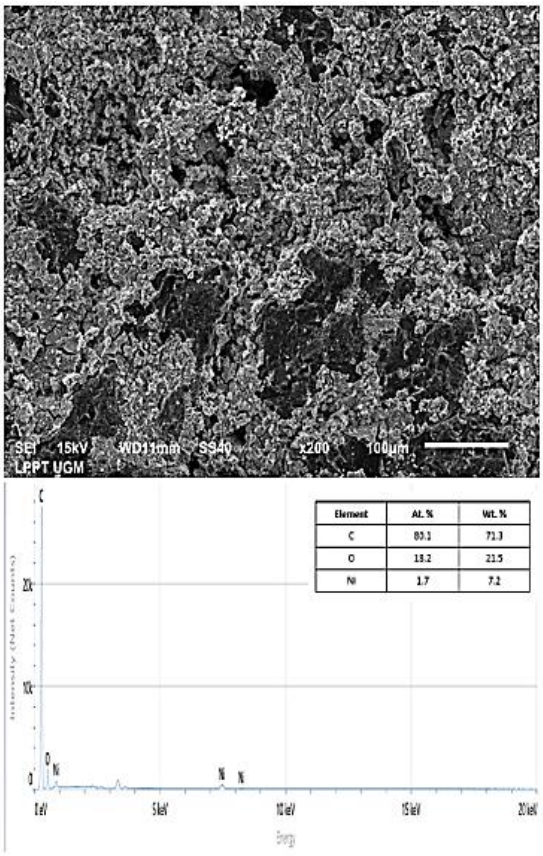


Fig. 3: SEM-EDX of graphite/NiO/G-OH

The decrease in absorbance at 595 nm indicates the degradation of the auxochrome (–N=N–) group in RB5. Meanwhile, the reduction in absorbance in the UV region at 229, 254, 310, and 391 nm suggests the breakdown of the benzene ring structure and the disruption of the conjugated system in the phenothiazine species (Shetti *et al.*, 2019). A smaller decrease in absorbance in the UV

region than in the visible region was observed (Figures 4, 5, and 6), because the aromatic structure is more stable than the auxochrome group. The electro-degradation of RB5 proceeds through both direct and indirect anodic oxidation mechanisms (Särkkä *et al.*, 2015). In direct oxidation, hydroxyl radicals are generated on the anode surface. In contrast indirect oxidation produces chlorine, hypochlorous acid, and hypochlorite ions, or hydrogen peroxide and ozone, formed on the electrode according to the following reaction equations:

$$2Cl^- \rightarrow Cl_2 + 2e^- \quad (1)$$

$$Cl_2 + H_2O \rightarrow HOCl + H^+ + Cl^- \quad (2)$$

$$HOCl \rightarrow H^+ + OCl^- \quad (3)$$

$$H_2O \rightarrow \bullet OH + H^+ + e^- \quad (4)$$

$$2 \bullet OH \rightarrow H_2O_2 \quad (5)$$

$$H_2O_2 \rightarrow O_2 + 2H^+ + 2e^- \quad (6)$$

$$O_2 + \bullet O \rightarrow O_3 \quad (7)$$

Direct anodic oxidation is more advantageous than indirect oxidation because it does not require the addition of external chemicals to the solution and generates fewer secondary pollutants (Feng *et al.*, 2019). The incorporation of G–OH as a modifier material on the graphite electrode facilitates the generation of hydroxyl radicals, which act as strong oxidizing agents, as shown in reactions (8) and (9).

$$G\text{-}OH \rightarrow G\text{-}O\bullet + H^+ + e^- \quad (8)$$

$$G\text{-}O\bullet + OH^- \rightarrow G\text{-}O^- + \bullet OH \quad (9)$$

The main mechanism of organic compound degradation using the graphite/NiO/G–OH anode involves the formation of hydroxyl radicals (•OH), which are strong oxidizing agents (reactions 8 and 9). The coating with reduced graphene oxide (rGO), known for its excellent electrocatalytic properties, is expected to enhance the conductivity of the graphite/NiO/G–OH anode and increase the formation of oxidizing species such as Cl_2 and •OH. When NaCl is used as the supporting electrolyte, reactions 8–11 may occur during electro-degradation.

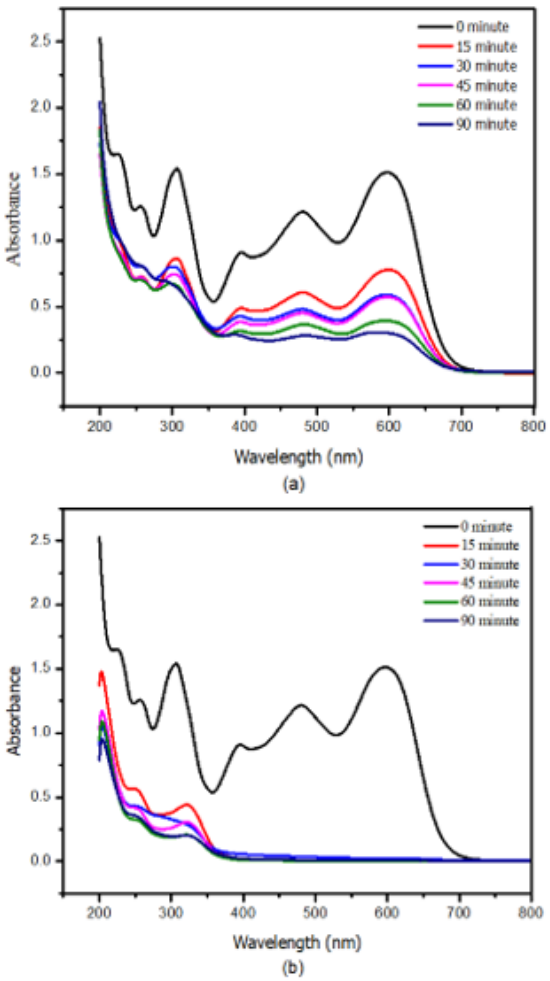


Fig. 4: Absorbance spectra of RB5 at different electro-degradation times using (a) graphite and (b) graphite/NiO/G–OH electrodes

$$rG\text{-}O\bullet + Cl^- \rightarrow rG\text{-}O^- + Cl\bullet \quad (10)$$

$$Cl\bullet + Cl^- \rightarrow Cl_2 + e^- \quad (11)$$

$$RB5 + OCl^- \rightarrow CO_2 + H_2O + Cl^- \quad (12)$$

$$RB5 + \bullet OH \rightarrow CO_2 + nH^+ + ne^- \quad (13)$$

Figures 1-3 show the deposition of NiO and G–OH on the surface of the graphite electrode. Electrodeposition of the NiO/G–OH electrocatalyst onto the graphite electrode enhances its ability to oxidize Cl^- (reaction 1) and accelerates the reactions described in reactions 2 and 3, thereby increasing the degradation efficiency of RB5 (reaction 12). The other, electrodeposition of NiO/G–OH electrocatalyst on a graphite electrode increases •OH production (reactions 8 and 9), thereby enhancing the direct electrooxidation of RB5 (reaction 13).

Figure 4 shows that the electro-degradation time significantly affects the degradation efficiency. In this study, the reaction time was optimized at 15, 30, 45, 60, and 90 minutes with an initial RB5 concentration of 300 ppm, a voltage of 9 V, 0.05 M NaCl, and pH 8. Based on Figure 4, the optimum electro-degradation time was achieved at 60 minutes, with degradation efficiencies of 98.75% for the graphite/NiO/G–OH electrode and 74.50% for the graphite electrode.

The findings indicate that increasing the electro-degradation time leads to a higher concentration of major oxidizing agents, namely hydroxyl radicals (•OH) and chlorine species, which play a key role in dye degradation (Pereira *et al.*, 2020). Previous studies have reported similar trends. For instance, the decolorization efficiency of methylene blue using a G/β-PbO_2 electrode increased from 79.67% after 10 minutes to 97.67% after 50 minutes of electro-degradation (Samarghandi *et al.*, 2020). Likewise, platinum (Pt) electrodes achieved 88.68% reduction in the absorbance of Active Blue 21 dye within 5 minutes, which further increased to 99.94% after 20 minutes of electro-degradation (Aggadi *et al.*, 2021).

Electro-degradation of RB5 at different pH levels was carried out at the optimum reaction time of 60 minutes (Figure 5). The absorbance spectra at pH 4, 6, and 8 showed no significant changes, indicating relatively stable degradation behavior across these pH values. However, the greatest decrease in absorbance was observed at pH 4 for both graphite and graphite/NiO/G–OH electrodes, with electro-degradation efficiencies of 78.96% and 99.87%, respectively. Under acidic conditions, free chlorine (HClO) is the dominant oxidizing agent, whereas at slightly alkaline conditions, hypochlorite (ClO^-) and chloride (Cl^-) ions are more prevalent. At pH 4, the concentration of HClO is higher than that of ClO^-, and HClO acts as a stronger oxidizing agent (Sandoval *et al.*, 2019). In

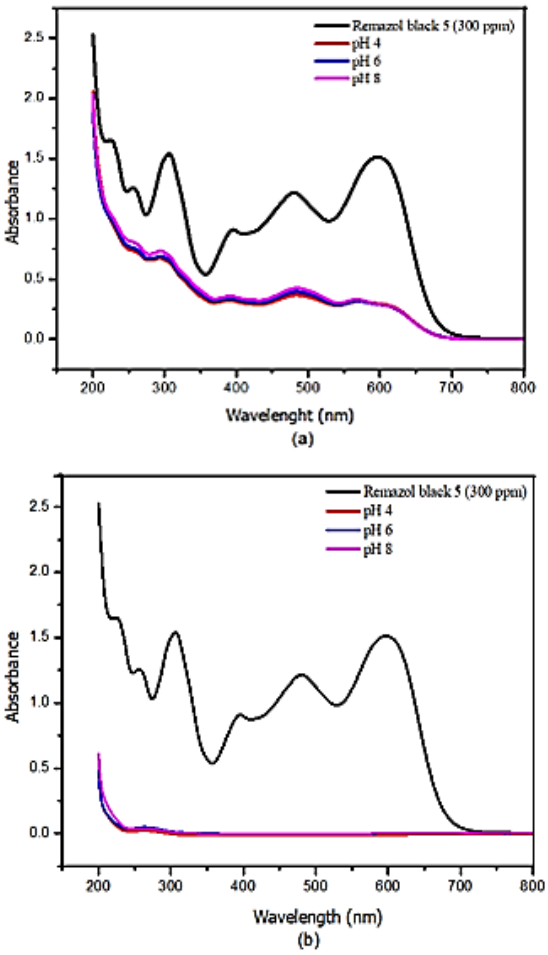


Fig. 5: Absorbance spectra of RB5 at different pH levels during electro-degradation using (a) graphite and (b) graphite/NiO/G–OH electrodes

addition, rGO contains fewer oxygen-containing functional groups, making it relatively stable under various pH conditions (Pieczynska *et al.*, 2019; Moreira *et al.*, 2017; Moreno-Palacios *et al.*, 2019; Yao *et al.*, 2021).

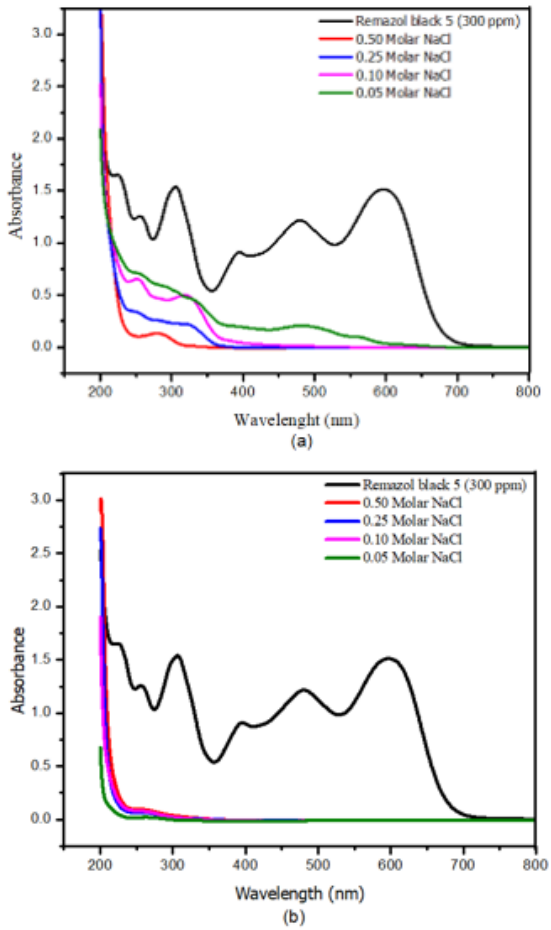


Fig. 6: Absorbance spectra of RB5 at different NaCl concentrations using (a) graphite and (b) graphite/NiO/G–OH electrodes

Previous studies reported that the electro-degradation of Acid Blue 80 using BDD and platinum anodes proceeded more rapidly under acidic conditions, whereas at alkaline pH (pH 11) the degradation rate was slower (Kuchtová *et al.*, 2020). Similarly, the degradation of Acid Yellow 25 dye using $Ti/Ru_{0.3}Ti_{0.7}O_2$ electrodes achieved a COD removal efficiency of 74% at pH 3 and 58% at pH 10 (Sandoval *et al.*, 2019).

Electro-degradation of RB5 at different NaCl concentrations was carried out under the optimum conditions of pH 4 and a reaction time of 60 minutes (Figure 6). The results show that the optimum NaCl concentration for the electro-oxidation of RB5 was 0.50 M when using the graphite electrode, and 0.05 M when using the graphite/NiO/G–OH electrode. The absorbance spectra of RB5 electro-degradation using the graphite/NiO/G–OH electrode showed a significantly greater decrease compared to the graphite electrode. At a NaCl concentration of 0.05 M, the electro-degradation efficiency for RB5 was 80.30% using graphite and 100% using the graphite/NiO/G–OH electrode.

The use of NaCl solution as a supporting electrolyte in the presence of G–OH facilitates the oxidation of Cl^- to Cl_2, which subsequently forms other strong oxidizing species such as chlorine and hypochlorite ions on the electrode surface. This process enhances the effectiveness of the electrochemical degradation of organic compounds. Based on these findings, graphite/NiO/G–OH exhibits strong potential as an electrocatalyst for the electro-degradation of RB5 (Samarghandi *et al.*, 2020). The optimum conditions for the electro-degradation of RB5 using a graphite electrode were obtained at pH 4, NaCl concentration of 0.10 M, and a reaction time of 60 minutes, with an absorbance reduction efficiency of 94.05%. Meanwhile, for the graphite/NiO/G–OH electrode, the optimum conditions were pH 4, NaCl concentration of 0.05 M, and 60 minutes of electro-degradation time, achieving an absorbance reduction efficiency of 100%.

Previous research reported that the degradation efficiency increased from 64.77% to 93.60% with increasing NaCl concentration

during the electrolysis of 1 $g{\cdot}L^{-1}$ reactive red dye using RuO_2–IrO_2/Ti electrodes over a 3-hour degradation process (Yao *et al.*, 2021). Similarly, the degradation efficiency also increased with increasing Na_2SO_4 concentration during the electrochemical oxidation of acid orange 7 azo dye using a PbO_2 electrode (Xia *et al.*, 2019).

Table 1 summarizes the results of previous studies on the electrochemical oxidation of textile dyes using various anode materials. Differences in removal efficiency values are caused by variations in the electrochemically generated oxidant, electrode material, applied current, and electrolyte solution (Jinisha *et al.*, 2018). Electro-degradation of RB5 using the graphite/NiO/G–OH electrode showed higher absorbance reduction efficiency compared to GN/TiO_2 and G/NiO/Ni electrodes. Therefore, the graphite/NiO/G–OH electrode is effective for the electrochemical removal of RB5. The deposition of the NiO/G–OH electrocatalyst on the surface of the graphite electrode (Figures 1–3) increased the electrode potential for Cl^- oxidation (reaction 1) and accelerated reactions (12) and (13), resulting in 100% absorbance reduction efficiency.

GC–MS analysis was conducted to identify the intermediates formed in the liquid phase during the electro-degradation of RB5. The appearance of intermediate products indicates that the electrooxidation of RB5 using graphite/NiO/G-OH electrodes occurs in two steps. First, RB5 molecules react

Table 1. Electrochemical dye removal using various electrodes reported in the literature

No.	Dye	E	A	C	A.Ef	Ref.
1	RV-2 dye (100 ppm)	E.time 60 min, j = 79 $A.m^2$, NaCl = $g.L^{-1}$, pH = 7	G	SS	95%	(Hamad *et al.*, 2018)
	AB-14 dye (100 ppm)				69.8%	
2	RBk5 (10 ppm)	E.time 60 min, j = 2.5 $mA.cm^2$, NaCl = 1 $g.L^{-1}$, pH = 6.6	GN/TiO_2	Cu	>95%	(Li *et al.*, 2019)
3	MB dye (60 ppm)	E.time 50 min, j = 10 $mA.cm^2$, Na_2SO_4 = 78.8 $mg.L^{-1}$, pH = 5.75	G/PbO_2	SS	96.2%	(Samarghandi *et al.*, 2020)
			G	SS	68.3%	
4	MB (25 ppm)	E.time 12 min, j = 10 $mA.cm^2$, Na_2SO_4 = 0.5 mol L^{-1}	GN/SnO_2	Pt	35%	(Sharif & Roberts, 2020)
			GN/Sb-SnO_2	Pt	40%	
5	MB (20 ppm)	E.time 30 min, j = 20 $mA.cm^2$, NaCl = 0.05 M, pH = 3	SS/G-OH	SS	>99%	(Yusbarina *et al.*, 2021)
6	RB-5 (100 ppm)	E.time 60 min, V = 9 volt, NaCl = 0.05 M, pH = 4	G/NiO/Ni	G	100%	(Wiratini *et al.*, 2023)
7	RB-5 (300 ppm)	E.time 60 min, V = 9 volt, NaCl = 0.10 M	G	G	94.05%	This work
		E.time 60 min, V = 9 volt, NaCl = 0.05 M	G/NiO/G–OH	G	100%	

E: Experimental conditions, A: Anode, C: Cathode, A.Ef: Absorbance removal efficiency, E.time: Electrochemical removal time, G: Graphite, GN: Graphene, SS: Stainless steel

with •OH radicals and dissolved oxidizing agents (Cl_2 and HOCl) to produce smaller linear molecules. Second, these small molecules are further degraded to produce CO_2 and H_2O. The intermediates detected after 60 minutes of electrooxidation are presented in Table 2 and Figure 7. The results reveal three dominant peaks at retention times of 6.07, 14.24, and 29.23 minutes, all of which decreased after the electro-degradation process using the graphite/NiO/G-OH electrode (Figure 7b). The decrease in the peak at 29.23 minutes indicates that the deposition of the NiO/G-OH electrocatalyst enhances the mineralization of the RB5 dye.

Table 2. GC–MS results of RB5 after 60 minutes of electro-degradation using graphite and graphite/NiO/G-OH electrodes

No	Retention time (minutes)	Graphite	Graphite/ NiO/G-OH
1	6.07	$C_{12}H_{20}O_2$	$C_{12}H_{20}O_2$
2	10.6	$C_{15}H_{24}O$	$C_{15}H_{24}O$
3	14.24	$C_{11}H_{14}O_3$	$C_{11}H_{14}O_3$
4	26.21	$C_{35}H_{68}O_5$	
5	29.16	$C_{16}H_{28}$	$C_{15}H_{26}O_2$
		$C_{15}H_{28}O$	$C_{15}H_{28}O$
6	29.23	$C_{18}H_{36}O$	$C_{18}H_{36}O$
		$C_{18}H_{34}O_2$	
		$C_{18}H_{34}O$	$C_{18}H_{34}O$
7	29.62	$C_{39}H_{76}O_5$	$C_{39}H_{76}O_5$
		$C_{35}H_{68}O_5$	$C_{35}H_{68}O_5$
8	31.48	$C_{23}H_{50}O_3$	

Based on the GC–MS spectra, the possible electro-degradation products from the partial oxidation of RB5 include cyclic compounds, aromatic compounds, and organic acids. These results are consistent with the UV–Vis findings (Figures 4–5), indicating that the azo chromophore was no longer detected, while unsaturated groups were still present in the GC–MS spectra. The detection of a single benzene ring suggests that RB5 was degraded by •OH radicals and other oxidants such as Cl_2, ClO^-, and HOCl. Subsequently, the cyclic compounds were further broken down into single-ring structures, which were then oxidized and mineralized into smaller molecular products that ultimately degraded into CO_2 and H_2O.

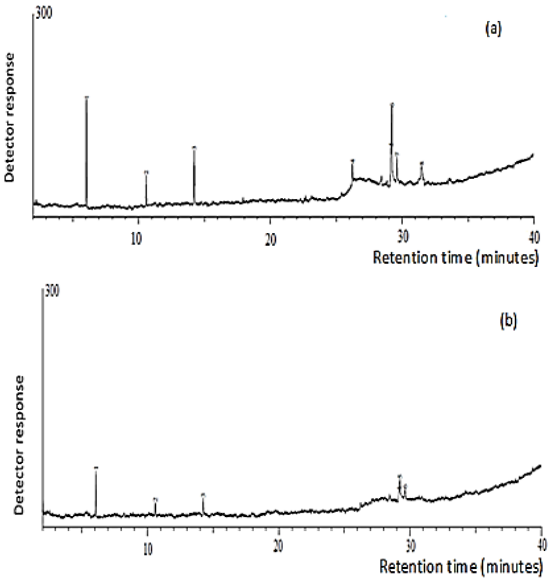


Fig. 7: GC–MS spectra of RB5 after 60 minutes of electrooxidation using (a) graphite and (b) graphite/NiO/G-OH electrodes

Previous research reported that the GC–MS analysis of MB degradation intermediates revealed the formation of organic acids (Wang *et al.*, 2018). GC–MS analysis of the electrochemical degradation of acid orange 7 using an ACF/Fe (activated carbon fiber) anode and an ACF/Ti cathode after 60 minutes of electrolysis identified heterocyclic compounds, naphthalene, and aromatic compounds as intermediate products. The electrolytic decomposition of acid orange 7 follows a degradation pathway in which aromatic intermediates are further oxidized

into open-ring products and eventually mineralized into CO_2, H_2O, and inorganic salts (Zhao *et al.*, 2010).

CONCLUSIONS

The graphite/NiO/G-OH electrode was successfully synthesized through the preparation of G-OH using electrochemical exfoliation followed by ultrasonication. Subsequently, G-OH and NiO were electrodeposited onto the graphite substrate. FTIR analysis confirmed the presence of characteristic functional groups, with peaks at 1,635 cm^{-1} corresponding to C=C and H–O–H stretching vibrations, and a peak at 1,126 cm^{-1} indicating C–O bonding. The peaks at 700 cm^{-1} and 501 cm^{-1} were attributed to Ni^{2+}–OH and Ni–O stretching vibrations, respectively. SEM–EDX analysis verified the deposition of C, O, and Ni elements on the graphite surface. The electro-degradation efficiency of RB5 reached 80.30% using graphite and 100% using the graphite/NiO/G-OH electrode. GC–MS analysis revealed that the electrooxidation products of RB5 consisted of cyclic compounds, aromatic compounds, and organic acids.

ACKNOWLEDGEMENT

This research was supported by the Ganesha University of Education under the Basic Research Scheme for the Fiscal Year 2024, Grant Number: 1129/UN48.16/LT/2024.

REFERENCES

Aggadi, S. El, Abbassi, Z. El, and Hourch, A. El, 2021. "Color Removal from Dye-Containing Aqueous Solutions by Electrooxidation." *Desalin. Water Treat., 215*, 232–236. https://doi.org/10.5004/dwt.2021.26766

Ajeel, M.A., Aroua, M.K.T., and Daud, W.M.A.W., 2016. "Reactivity of Carbon Black Diamond Electrode During the Electro-oxidation of Remazol Brilliant Blue R." *RSC Adv., 6*, 3690–3699. https://doi.org/10.1039/c5ra21487d

Basharat, F., Rana, U.A., Shahid, M., and Serwar, M., 2015. "Heat Treatment of Electrodeposited NiO Films for Improved Catalytic Water Oxidation." *RSC Adv., 5*, 86713–86722. https://doi.org/10.1039/c5ra17041a

Bravo-Yumi, N., Espinoza-Montero, P., Picos-Benítez, A., Navarro-Mendoza, R., Brillas, E., and Peralta-Hernández, J.M., 2020. "Synthesis and Characterization of Sb_2O_5-Doped Ti/SnO_2-IrO_2 Anodes Toward Efficient Degradation Tannery Dyes by in Situ Generated Oxidizing Species." *Electrochim. Acta, 358*, 136904. https://doi.org/10.1016/j.electacta.2020.136904

Brillas, E., and Martínez-Huitle, C.A., 2015. "Decontamination of Wastewaters Containing Synthetic Organic Dyes by Electrochemical Methods. An updated review." *Appl. Catal. B Environ., 166–167*, 603–643. https://doi.org/10.1016/j.apcatb.2014.11.016

Chow, D., Burns, N., Boateng, E., van der Zalm, J., Kycia, S., and Chen, A., 2023. "Mechanical Exfoliation of Expanded Graphite to Graphene-Based Materials and Modification with Palladium Nanoparticles for Hydrogen Storage." *Nanomaterials, 13*, 2588. https://doi.org/10.3390/nano13182588

Cornejo, O.M., Murrieta, M.F., Castañeda, L.F., and Nava, J.L., 2019. "Characterization of The Reaction Environment in Flow

Reactors Fitted with BDD Electrodes for Use in Electrochemical Advanced Oxidation Processes: A Critical Review." *Electrochim. Acta, 331*. https://doi.org/10.1016/j.electacta.2019.135373

Dar, F.I., Moonooswamy, K.R., and Es-Souni, M., 2013. "Morphology and Property Control of NiO Nanostructures for Supercapacitor Applications." *Nanoscale Res. Lett., 8*, 1–7. https://doi.org/10.1186/1556-276X-8-363

Ding, R., Li, X., Shi, W., Xu, Q., Wang, L., Jiang, H., Yang, Z., and Liu, E., 2016. "Mesoporous Ni-P Nanocatalysts for Alkaline Urea Electrooxidation." *Electrochim. Acta, 222*, 455–462. https://doi.org/10.1016/j.electacta.2016.10.198

Droguett, T., Mora-Gómez, J., García-Gabaldón, M., Ortega, E., Mestre, S., Cifuentes, G., and Pérez-Herranz, V., 2020. "Electrochemical Degradation of Reactive Black 5 Using Two-Different Reactor Configuration." *Sci. Rep., 10*, 1–11. https://doi.org/10.1038/s41598-020-61501-5

Feng, Z., Li, D., Wang, L., Sun, Q., Lu, P., Xing, P., and An, M., 2019. "A 3D Porous Ni-Zn/RGO Catalyst with Superaerophobic Surface for High-Performance Hydrazine Electrooxidation." *J. Alloys Compd., 788*, 1240–1245. https://doi.org/10.1016/j.jallcom.2019.03.007

Gündüz, Z., and Atabey, M., 2019. "Effects of Operational Parameters on the Decolourisation of Reactive Red 195 Dye from Aqueous Solutions by Electrochemical Treatment." *Int. J. Electrochem. Sci., 14*, 5868–5885. https://doi.org/10.20964/2019.06.37

Hamad, H., Bassyouni, D., El-Ashtoukhy, E.S., Amin, N., and Abd El-Latif, M., 2018. "Electrocatalytic Degradation and Minimization of Specific Energy Consumption of Synthetic Azo Dye from Wastewater by Anodic Oxidation Process with an Emphasis on Enhancing Economic Efficiency and Reaction Mechanism." *Ecotoxicol. Environ. Saf., 148*, 501–512. https://doi.org/10.1016/j.ecoenv.2017.10.061

Htwe, Y.Z.N., Chow, W.S., Suda, Y., Thant, A.A., and Mariatti, M., 2019. "Effect of Electrolytes and Sonication Times on the Formation of Graphene Using an Electrochemical Exfoliation Process." *Appl. Surf. Sci., 469*, 951–961. https://doi.org/10.1016/j.apsusc.2018.11.029

Jinisha, R., Gandhimathi, R., Ramesh, S.T., Nidheesh, P. V., and Velmathi, S., 2018. "Removal of Rhodamine B Dye from Aqueous Solution by Electro-Fenton Process Using Iron-doped Mesoporous Silica as a Heterogeneous Catalyst." *Chemosphere, 200*, 446–454. https://doi.org/10.1016/j.chemosphere.2018.02.117

Jung, W.T., Jang, H.S., Jeon, J.W., and Kim, B.H., 2021. "Effect of Oxygen Functional Groups in Reduced Graphene Oxide-Coated Silk Electronic Textiles for Enhancement of NO_2 Gas-Sensing Performance." *ACS Omega 6*, 27080–27088. https://doi.org/10.1021/acsomega.1c03658

Kaur, P., Kushwaha, J.P., and Sangal, V.K., 2018. "Transformation Products and Degradation Pathway of Textile Industry Wastewater Pollutants in Electro-Fenton Process." *Chemosphere, 207*, 690–698.

https://doi.org/10.1016/j.chemosphere.2018.05.114

Kim, Y.G., and Jo, W.K., 2019. "Efficient Decontamination of Textile Industry Wastewater Using a Photochemically Stable n–n Type CdSe/Ag_3PO_4 Heterostructured Nanohybrid Containing Metallic Ag as a Mediator." *J. Hazard. Mater., 361*, 64–72. https://doi.org/10.1016/j.jhazmat.2018.08.074

Kuchtová, G., Chýlková, J., Váňa, J., Vojs, M., and Dušek, L., 2020. "Electro-Oxidative Decolorization and Treatment of Model Wastewater Containing Acid Blue 80 on Boron Doped Diamond and Platinum Anodes." *J. Electroanal. Chem., 863*. https://doi.org/10.1016/j.jelechem.2020.114036

Li, J., Guan, Q., Hong, J., and Chang, C.-T., 2019. "Electrochemical Oxidation of Azo Dye Wastewater Using Graphene-Based Electrode Materials." *J. Nanosci. Nanotechnol., 19*, 7308–7314. https://doi.org/10.1166/jnn.2019.16656

Li, L., Yao, J., Fang, X., Huang, Y., and Mu, Y., 2017. "Electrolytic Ammonia Removal And Current Efficiency by A Vermiculite-Packed Electrochemical Reactor." *Sci. Rep., 7*, 1–8. https://doi.org/10.1038/srep41030

Migliorini, F.L., Steter, J.R., Rocha, R.S., Lanza, M.R.V., Baldan, M.R., and Ferreira, N.G., 2016. "Efficiency Study and Mechanistic Aspects in The Brilliant Green Dye Degradation Using BDD/Ti Electrodes." *Diam. Relat. Mater., 65*, 5–12. https://doi.org/10.1016/j.diamond.2015.12.013

Moreira, F.C., Boaventura, R.A.R., Brillas, E., and Vilar, V.J.P., 2017. "Electrochemical Advanced Oxidation Processes: A Review on Their Application to Synthetic and Real Wastewaters." *Appl. Catal. B Environ., 202*, 217–261. https://doi.org/10.1016/j.apcatb.2016.08.037

Moreno-Palacios, A. V., Palma-Goyes, R.E., Vazquez-Arenas, J., and Torres-Palma, R.A., 2019. "Bench-scale Reactor for cefadroxil Oxidation and Elimination of Its Antibiotic Activity Using Electro-Generated Active Chlorine." *J. Environ. Chem. Eng., 7*, 103173. https://doi.org/10.1016/j.jece.2019.103173

Nidheesh, P. V., Zhou, M., and Oturan, M.A., 2018. "An Overview on The Removal of Synthetic Dyes from Water by Electrochemical Advanced Oxidation Processes." *Chemosphere, 197*, 210–227. https://doi.org/10.1016/j.chemosphere.2017.12.195

Parvez, K., Wu, Z.S., Li, R., Liu, X., Graf, R., Feng, X., and Müllen, K., 2014. "Exfoliation of Graphite Into Graphene in Aqueous Solutions of Inorganic Salts." *J. Am. Chem. Soc. 136*, 6083–6091. https://doi.org/10.1021/ja5017156

Parvez, K., Yang, S., Feng, X., and Müllen, K., 2015. "Exfoliation of Graphene Via Wet Chemical Routes." *Synth. Met., 210*, 123–132. https://doi.org/10.1016/j.synthmet.2015.07.014

Pereira, L.A., de Lima Almeida, D.A., Couto, A.B., and Ferreira, N.G., 2020. "Titanium Dioxide/Oxidized Carbon Fiber Electrodes Electrochemically Produced and their Influences on Brilliant Green Dye Degradation." *Mater. Res. Bull., 122*, 110642. https://doi.org/10.1016/j.materresbull.2019.110642

Pieczyńska, A., Ossowski, T., Bogdanowicz, R., and Siedlecka, E., 2019. "Electrochemical

Degradation of Textile Dyes in A Flow Reactor: Effect of Operating Conditions and Dyes Chemical Structure." *Int. J. Environ. Sci. Technol., 16*, 929–942. https://doi.org/10.1007/s13762-018-1704-0

Ramalingam, S., 2019. "Nano SiC Reinforced Copper Nanocomposite by a Simple Electrodeposition Method." *Int. J. Eng. Adv. Technol., 9*, 239–244. https://doi.org/10.35940/ijeat.a1153.1291s419

Rebelo, Q.H.F., Ferreira, C.S., Santos, P.L., Bonacin, J.A., Passos, R.R., Pocrifka, L.A., and Paula, M.M.S., 2019. "Synthesis and Characterization of A Nanocomposite NiO/SiO_2 from A Sustainable Source of SiO_2." *Part. Sci. Technol., 37*, 907–911. https://doi.org/10.1080/02726351.2018.1455781

Rivera, M., Pazos, M., and Sanromán, M.Á., 2011. "Development of an Electrochemical Cell for The Removal of Reactive Black 5." *Desalination, 274*, 39–43. https://doi.org/10.1016/j.desal.2011.01.074

Safarpour, M., and Khataee, A., 2018. Graphene-Based Materials for Water Purification. Nanoscale Materials in Water Purification. Elsevier Inc. https://doi.org/10.1016/B978-0-12-813926-4.00021-5

Samarghandi, M.R., Dargahi, A., Shabanloo, A., Nasab, H.Z., Vaziri, Y., and Ansari, A., 2020. "Electrochemical Degradation of Methylene Blue Dye Using A Graphite Doped PbO_2 Anode: Optimization of Operational Parameters, Degradation Pathway and Improving The Biodegradability of Textile Wastewater." *Arab. J. Chem., 13*, 6847–6864. https://doi.org/10.1016/j.arabjc.2020.06.038

Sandoval, M.A., Zúñiga-Mallea, N., Espinoza, L.C., Vidal, J., Jara-Ulloa, P., and Salazar, R., 2019. "Decolorization and Degradation of a Mixture of Industrial Azo Dyes by Anodic Oxidation Using a Ti/$Ru0.3Ti_{0.7}O_2$ (DSA-Cl_2) Electrode." *Chemistry Select, 4*, 13856–13866. https://doi.org/10.1002/slct.201903150

Särkkä, H., Bhatnagar, A., and Sillanpää, M., 2015. "Recent Developments of Electro-Oxidation in Water Treatment - A review." *J. Electroanal. Chem., 754*, 46–56. https://doi.org/10.1016/j.jelechem.2015.06.016

Sharif, F., and Roberts, E.P.L., 2020. "Electrochemical Oxidation of An Organic Dye Adsorbed on Tin Oxide and Antimony Doped Tin Oxide Graphene Composites." *Catalysts, 10*. https://doi.org/10.3390/catal10020263

Shestakova, M., and Sillanpää, M., 2017. "Electrode Materials Used for Electrochemical Oxidation of Organic Compounds in Wastewater." *Rev. Environ. Sci. Biotechnol., 16*, 223–238. https://doi.org/10.1007/s11157-017-9426-1

Shetti, N.P., Malode, S.J., Malladi, R.S., Nargund, S.L., Shukla, S.S., and Aminabhavi, T.M., 2019. "Electrochemical Detection and Degradation of Textile Dye Congo Red At Graphene Oxide Modified Electrode." *Microchem. J., 146*, 387–392. https://doi.org/10.1016/j.microc.2019.01.033

Tang, Y., He, D., Guo, Y., Qu, W., Shang, J., Zhou, L., Pan, R., and Dong, W., 2020. "Electrochemical Oxidative Degradation of X-6G Dye by Boron-Doped Diamond Anodes: Effect of Operating Parameters." *Chemosphere, 258*, 127368.

https://doi.org/10.1016/j.chemosphere.2020.127368

Thaneswari, S.A., and Lourduraj, A.J.C., 2017. "Facile Single Step Electrochemical Synthesis of Few Layered Graphene for energy storage Applications." *Arab. J. Chem., 18*, 80–84.

Vacchi, I.A., Raya, J., Bianco, A., and Ménard-Moyon, C., 2018. "Controlled Derivatization of Hydroxyl Groups of Graphene Oxide in Mild Conditions." *2D Mater., 5*. https://doi.org/10.1088/2053-1583/aac8a9

Vasconcelos, V.M., Ponce-de-León, C., Rosiwal, S.M., and Lanza, M.R.V., 2019. "Electrochemical Degradation of Reactive Blue 19 Dye by Combining Boron-Doped Diamond and Reticulated Vitreous Carbon Electrodes." *Chem, Electro. Chem., 6*, 3516–3524. https://doi.org/10.1002/celc.201900563

Wang, X.Q., Han, S.F., Zhang, Q.W., Zhang, N., and Zhao, D.D., 2018. "Photocatalytic Oxidation Degradation Mechanism Study of Methylene Blue Dye Waste Water with GR/iTO$_2$." *MATEC Web Conf., 238*. https://doi.org/10.1051/matecconf/201823803006

Wiratini, N.M., Trisunaryanti, W., Triyono, and Kuncaka, A., 2023. "Electrochemical Removal of Remazol Black 5 (RB-5) Using SiO_2/NiO/Ni Nanocomposite Electrocatalyst Deposited on the Surface of Graphite Electrodes." *Evergreen, 10*, 1274–1285. https://doi.org/10.5109/7151673

Xia, Y., Wang, G., Guo, L., Dai, Q., and Ma, X., 2019. "Electrochemical Oxidation Of Acid Orange 7 Azo Dye Using a PbO_2 Electrode: Parameter Optimization, Reaction Mechanism and Toxicity Evaluation." *Chemosphere, 241*, 125010. https://doi.org/10.1016/j.chemosphere.2019.125010

Yan, L., Lin, M., Zeng, C., Chen, Z., Zhang, S., Zhao, X., Wu, A., Wang, Y., Dai, L., Qu, J., Guo, M., and Liu, Y., 2012. "Electroactive and Biocompatible Hydroxyl-Functionalized Graphene by Ball Milling." *J. Mater. Chem., 22*, 8367–8371. https://doi.org/10.1039/c2jm30961k

Yao, Y., Chen, Q., and Zhou, J., 2021. "Influence of Typical Electrolytes on Electrooxidation of Bio-Refractory Reactive Dye." *Int. J. Environ. Sci. Technol., 19*, 1799–1810. https://doi.org/10.1007/s13762-021-03184-7

Yusbarina, Y., Roto, R., and Triyana, K., 2021. "Hydroxyl Functionalized Graphene As a Superior Anode Material for Electrochemical Oxidation of Methylene Blue." *Rasayan J. Chem., 14 (2)*, 1140–1147. https://doi.org/10.31788/rjc.2021.1426180

Zhang, J., Zhang, D., and Liu, Y., 2019. "Ni–SiO2 Nanoporous Composite as an Efficient Electrocatalyst for the Electrooxidation of Hydrogen Peroxide." *J. Mater. Sci. Mater. Electron., 30*, 13895–13909. https://doi.org/10.1007/s10854-019-01707-0

Zhao, H.Z., Sun, Y., Xu, L.N., and Ni, J.R., 2010. "Removal of Acid Orange 7 in Simulated Wastewater Using a Three-Dimensional Electrode Reactor: Removal Mechanisms and Dye Degradation Pathway." *Chemosphere, 78*, 46–51. https://doi.org/10.1016/j.chemosphere.2009.10.034.